HHS Public Access

Author manuscript

Eur Urol Oncol. Author manuscript; available in PMC 2021 July 02.

Published in final edited form as:

Eur Urol Oncol. 2018 October ; 1(5): 364–377. doi:10.1016/j.euo.2018.04.015.

Plasma Glycosaminoglycans as Diagnostic and Prognostic Biomarkers in Surgically Treated Renal Cell Carcinoma

Francesco Gatto[a,†], **Kyle A. Blum**[b], **Seyedeh Shaghayegh Hosseini**[a], **Mazyar Ghanaat**[b], **Mahyar Kashan**[b], **Francesca Maccari**[c], **Fabio Galeotti**[c], **James J. Hsieh**[d,‡], **Nicola Volpi**[c], **A. Ari Hakimi**[b], **Jens Nielsen**[a,*]

[a]Department of Biology and Biological Engineering, Chalmers University of Technology, Göteborg, Sweden

[b]Department of Surgery, Urology Service, Memorial Sloan Kettering Cancer Center, New York, NY, USA

[c]Department of Life Sciences, University of Modena and Reggio Emilia, Modena, Italy

[d]Department of Medicine, Genitourinary Oncology, Memorial Sloan Kettering Cancer Center, New York, NY, USA

Abstract

Background: Plasma glycosaminoglycan (GAG) measurements, when aggregated into diagnostic scores, accurately distinguish metastatic clear-cell renal cell carcinoma (RCC) from healthy samples and correlate with prognosis. However, it is unknown if GAG scores can detect RCC in earlier stages or if they correlate with prognosis after surgery.

Objective: To explore the sensitivity and specificity of plasma GAGs for detection of early-stage RCC and prediction of recurrence and death after RCC surgery.

Design, setting, and participants: This was a retrospective case-control study consisting of a consecutive series of 175 RCC patients surgically treated between May 2011 and February 2014 and 19 healthy controls.

*Corresponding author. Department of Biology and Biological Engineering, Chalmers University of Technology, Kemivägen 10, Göteborg SE41296, Sweden. Tel.: +46 31 7723804, nielsenj@chalmers.se (J. Nielsen).
†Current address: Elypta AB, Stockholm, Sweden.
‡Current address: Molecular Oncology, Siteman Cancer Center, Washington University School of Medicine, St. Louis, MO, USA.

Author contributions: Jens Nielsen had full access to all the data in the study and takes responsibility for the integrity of the data and the accuracy of the data analysis.
Study concept and design: Gatto, Nielsen.
Acquisition of data: Gatto, Blum, Ghanaat, Kashan, Maccari, Galeotti, Volpi, Hosseini.
Analysis and interpretation of data: Gatto.
Drafting of the manuscript: Gatto.
Critical revision of the manuscript for important intellectual content: Gatto, Nielsen, Blum, Hakimi, Hsieh.
Statistical analysis: Gatto.
Obtaining funding: Nielsen, Hakimi.
Administrative, technical, or material support: None.
Supervision: Nielsen, Hakimi, Hsieh, Volpi.
Other: None.

Appendix A. Supplementary data
Supplementary data associated with this article can be found, in the online version, at doi:10.1016/j.eururo.2016.04.035.
The trial is registered on ClinicalTrial.gov as NCT03471897.

Outcome measurements and statistical analysis: Plasma GAGs in preoperative and postoperative RCC and healthy samples were measured using capillary electrophoresis with laser-induced fluorescence in a single blinded laboratory. A discovery set was first analyzed to update the historical GAG score. The sensitivity of the new GAG score for RCC detection versus healthy subjects was validated using the remaining samples. The correlation of the new GAG score to histopathologic variables, overall survival, and recurrence-free survival was evaluated using nonparametric and log-rank tests and multivariable Cox regression analyses.

Results and limitations: The RCC cohort included 94 stage I, 58 stage II–III, and 22 stage IV cases. In the first discovery set ($n = 67$), the new GAG score distinguished RCC from healthy samples with an area under the receiver operating characteristic curve (AUC) of 0.999. In the validation set ($n = 108$), the GAG score achieved an AUC of 0.991, with 93.5% sensitivity. GAG scores were elevated in RCC compared to healthy samples, irrespective of and uncorrelated to stage, grade, histology, age, or gender. The total chondroitin sulfate concentration was an independent prognostic factor for both overall and recurrence-free survival (hazard ratios 1.51 and 1.25) with high concordance when combined with variables available at pathologic diagnosis (C-index 0.926 and 0.849) or preoperatively (C-index 0.846 and 0.736). Limitations of the study include its retrospective nature and moderate variability in GAG laboratory measurements.

Conclusions: Plasma GAGs are highly sensitive diagnostic and prognostic biomarkers in surgically treated RCC independent of stage, grade, or histology. Prospective validation studies on GAG scores for early detection, prediction, and surveillance for RCC recurrence are thus warranted.

Patient summary: In this study, we examined if a new molecular blood test can detect renal cell carcinoma in the early stages and predict if the cancer might relapse after surgery.

Keywords

Renal cell carcinoma; Diagnostic biomarkers; Prognostic biomarkers; Liquid biopsy

1. Introduction

Renal cell carcinoma (RCC) is the most common form of kidney cancer, and the ninth most common cancer type in the Western world, accounting for approximately 90 000 deaths globally every year [1,2]. RCC is largely asymptomatic, so it is estimated that 20–40% of all cases diagnosed are at the metastatic stage at presentation [3,4], which is considered invariably incurable. Surgery is generally offered as curative treatment in nonmetastatic RCC. However, approximately 20% of all these cases experience recurrence within 5 yr after surgery, and ~90% of all recurrences involve metastatic disease [4]. Even if up to 50% of recurrences are deemed potentially curable (ie, local, solitary, or oligometastatic recurrence), it has been estimated that currently only half of these cases are offered local treatment with curative intent [5,6]. Despite these data, there are no consensus guidelines on surveillance for subgroups of the RCC population at high risk of recurrence, and the standard technology for surveillance—medical imaging—is not practical or cost-effective for detection of recurrence over prolonged periods. The introduction of minimally invasive biomarkers in the routine clinical management of RCC could facilitate early detection, prediction of

recurrence, and surveillance of RCC, all cases for which higher chances of cure can be expected. However, despite extensive research [7], no plasma or urine biomarker has been introduced into the clinical management pathway for RCC [8,9].

We and others observed that genetic alterations specific to clear cell RCC (ccRCC) correlated with marked metabolic reprogramming in these cancer cells compared to other common epithelial cancers [10–13]. Using a systems biology approach, we observed in both retrospective and prospective series of metastatic ccRCC cases that the composition and levels of plasma and urine glycosaminoglycans (GAGs) were significantly altered compared to healthy samples [14]. In addition, GAG scores correlated with progression-free survival and overall survival (OS) in a prospective cohort of patients with metastatic ccRCC [15]. However, it is still unknown whether alterations in plasma and urine GAGs are limited to metastatic ccRCC or correlate with other histopathologic variables in RCC. In addition, it is unknown whether the GAG correlation with prognosis is limited to ccRCC patients treated with systemic therapy or apply to surgically treated RCC as well.

In this study, we profiled plasma GAGs in a large retrospective consecutive series of patients with a radiographic finding of a renal mass. Consistent with our previous study, we also used a control group of healthy volunteers for measurement of plasma GAGs. The primary endpoints were the specificity and sensitivity of plasma GAGs in the detection of RCC in preoperative samples in comparison to healthy individuals. We further analyzed how plasma GAGs varied according to stage, grade, and RCC histology, and after surgery. Finally, we estimated whether plasma GAGs correlate with prognosis after surgery, assessed as OS and recurrence-free survival (RFS).

2. Patients and methods

2.1. Study design

This study is reported in compliance with the STARD and REMARK guidelines. Additional information on the methods and a subset of anonymized data are made available in the Supplementary material. The study was registered on ClinicalTrial.gov as NCT03471897.

We used a retrospective case-control design. Clinical data collection and laboratory measurements were performed blinded to each other. Inclusion criteria were patients with radiographic finding of a renal mass and healthy volunteers without any history of malignancy. The key exclusion criterion was the absence of preoperative samples following filtering out of outliers and laboratory assay failures. Participants were enrolled at the Memorial Sloan Kettering Cancer Center (New York, NY, USA) between May 25, 2011 and February 18, 2014. Eligible participants were identified from radiographic findings and formed a consecutive series. For subjects with a renal mass, plasma samples were collected up to 50 d before primary surgery. A convenience subcohort of these subjects was followed longitudinally and samples were collected during a follow-up visit between 1 and 30 mo after first surgery. For healthy volunteers, plasma samples were collected from relatives of cancer patients and formed a random convenience cohort.

Ethics permission for the study was obtained from the institutional review board at the Memorial Sloan Kettering Cancer Center on November 5, 2012 (#12–237).

2.2. GAG measurements

Whole blood samples were collected in EDTA-coated tubes. The tubes were centrifuged (1100 × *g* for 10 min) and the plasma was extracted and collected in a separate tube. All samples were stored at −80 °C. Samples were shipped in dry ice. Laboratory measurements of the GAG profile quantified 19 independent properties: the total concentration of chondroitin sulfate (CS; μg/ml); total concentration of heparan sulfate (HS; μg/ml); total concentration of hyaluronic acid (HA; μg/ml); mass fraction of eight CS sulfation patterns (0s CS, 2s CS, 6s CS, 4s CS, 2s6s CS, 2s4s CS, 4s6s CS, and Tris CS); and the mass fraction of eight HS sulfation patterns (0s HS, 2s HS, 6s HS, Ns HS, Ns6s HS, Ns2s HS, 2s6s HS, and Tris HS). In addition, the charge of CS and HS and three additional CS ratios were calculated (6s/0s CS, 4s/0s CS, and 4s/6s CS). The overall GAG profile therefore consisted of 24 properties. These properties were measured using capillary electrophoresis with laser-induced fluorescence in a single blinded laboratory, as previously described [16–18].

2.3. Exploratory data analysis

Principal component analysis (PCA) and unsupervised hierarchical clustering [19] were performed for all preoperative RCC and healthy control samples using either CS-only or HS-only properties. The enrichment of selected histopathologic features in the emerging clusters was tested using the proportional equality test.

2.4. GAG scores

Two different scoring systems for selected properties in the plasma GAG profile were used: the previously developed GAG score [14] and the new GAG score derived in this study. For diagnostic use, the index test was defined as the test that classifies a subject as having RCC if the formula for the previous GAG score in a sample from that subject returns a score greater than the prespecified cutoff for plasma GAG scores. The cutoff was the numerical value maximizing the accuracy in the classification RCC versus healthy samples as determined in our previous study [14]. The index test was conducted for all preoperative RCC samples versus healthy controls from this cohort or versus healthy controls from historical cohorts [14]. The reference standard for defining a subject as having RCC was the pathology report, while healthy status was self-reported. Index test results were not available to the assessors of the reference standard. A prespecified variation of the previously developed GAG score omitting the Ns HS term was also tested.

In the case of the new GAG score, the formula was derived using penalized regression with Lasso [20], as previously described [14]. To this end, 38% of the total preoperative RCC samples were randomly selected to form a discovery set, together with the healthy controls from this or historical cohorts. The optimal cutoff for the new GAG score was then computed. For validation, the index test was redefined in terms of the new GAG score and cutoff and tested on the remaining 62% of the total preoperative RCC samples. Note that only the index test sensitivity could be validated in this manner.

2.5. Statistical analysis

The area under the receiver operating characteristic curve (AUC), sensitivity, specificity, and accuracy were computed for classification of individuals as RCC versus healthy as per the reference standard according to the index test. Missing data in the index test caused by laboratory assay failure were omitted. No other missing or indeterminate data in the index test and reference standards were observed.

The difference in each of the GAG properties included during feature selection between RCC and healthy groups, adjusted by cohort, was assessed using Bayesian estimation with a bivariate linear model [21,22].

The association with tumor grade, stage, size, and histological subtype was assessed by applying a Mann-Whitney test or t test to the linear regression coefficient for categorical or continuous variables, respectively. Statistical significance was set to $p < 0.05$. The minimum study sample size was 156 consecutive patients and 10 healthy subjects as determined by power calculations.

2.6. Survival analysis

Survival was calculated as the time between the date of first surgery and the event time. The event time was defined as right-censoring (date of last follow-up without the event), date of death in the case of OS, and date of recurrence in the case of RFS. Recurrence was defined as radiological evidence of one or more metastatic lesions. The end of the follow-up period was November 2017. The study was not powered specifically for survival analysis.

Univariate and multivariate survival analyses were performed by fitting a Cox proportional hazards model to relevant clinical variables and the log-rank statistical test was applied to determine the regression significance. We checked for severe overfitting by performing internal validation of Lasso-penalized multivariate models for OS and RFS using a bootstrapping algorithm (1000 bootstraps) to correct the original Somers' D rank correlation (D_{xy}) statistics. The corrected D_{xy} is transformed into the concordance index $\left(C_{\text{index}} = \frac{D_{xy}}{2} + 0.5\right)$.

One of the constituent GAG properties of the new GAG score, namely the total CS concentration (CS_{tot}), was also used to dichotomize patients into two groups: low versus high score. Kaplan-Meier survival curves were fitted for the two groups, and the statistical significance for survival difference was evaluated using the log-rank test, with $p < 0.05$ considered significant.

2.7. Reproducibility analysis

Technical replicates were performed on 80 samples from a quasi-random subset of 40 patients to encompass a pair of preoperative and postoperative samples for each patient while balancing RCC histologies and the presence of metastases at surgery in the subset. The coefficient of variability and least-squared linear regression was computed for the new GAG score in the original batch (first batch) versus the replicated batch (second batch).

3. Results

3.1. Patient characteristics

In total, 237 subjects were retrospectively enrolled for this study, 218 patients and 19 healthy volunteers, for a total of 470 plasma samples encompassing both preoperative and postoperative samples (Supplementary Figure 1). We excluded 13 samples (3%) because of laboratory assay failure and seven (1.5%) because they met the criteria as outliers. We further excluded 24 patients (11%) because the preoperative samples were either too old or not available. For three patients, two preoperative samples were obtained within 50 d from surgery, the oldest of which was discarded. Overall, 19 healthy volunteers and 194 patients with preoperative samples were included in the study. Of the 194 patients, 152 (78%) had at least one postoperative sample. The median time between surgery and postoperative sample collection was 32 d (interquartile range [IQR] 26–38, range 4–222). Overall, 365 samples were included in the study.

The median age at diagnosis in the patient cohort was 60 yr (IQR 52–67). The cohort was predominantly composed of males (69%; 134 males vs 60 females) and white Americans (90%). The most common pathologic diagnosis was RCC (n = 175 patients; 90%), followed by oncocytoma (n = 7; 4%) and angiomyolipoma (n = 6; 3%). There were two cases with other benign renal masses (1 medullary fibroma and 1 mixed epithelial stromal tumor) and four cases of other malignant renal masses, including three urothelial cell carcinomas. Since the rate of other renal masses was substantially lower than anticipated, this study did not achieve the statistical power to use these cases as controls, which were therefore excluded from subsequent analyses. The median age in the healthy cohort was 55 yr (IQR 50–60) and the group included six males and 13 females. Age was not significantly different between the cohorts (p = 0.173; Mann-Whitney test), but the proportion of males was significantly higher in the patient group than in the healthy group (p = 0.002; proportion equality test). Baseline characteristics for all the subjects are shown in Table 1.

Limited to the subcohort of 175 RCC cases, the demographic characteristics were similar to those for the patient cohort (Table 2). The most common histological subtype was ccRCC (n = 124; 71%). Of the remaining 51 non-ccRCC (nccRCC) cases, the most common histological subtype was papillary RCC (n = 26), followed by chromophobe RCC (n = 17). Most RCC cases involved localized disease (stage I; n = 94; 54%), with the vast majority of tumors of <4 cm in size (pT1a; n = 70). The remaining RCC cases were predominantly locally advanced disease (stage II or III; n = 58). Finally, there were 22 cases of advanced disease (stage IV, including 1 pT4N0M0). The baseline characteristics for the RCC subcohort are shown in Table 2.

3.2. Plasma GAG profiles in preoperative RCC versus healthy controls

The GAG profile, which encompasses the total concentration, disaccharide composition, and charge for CS, HS, and HA (total of 24 properties), was measured in plasma samples using capillary electrophoresis with laser-induced fluorescence in a single blinded laboratory, as previously described [16–18].

We performed PCA to ascertain in an unbiased fashion how similar the CS and HS profiles were across preoperative RCC and healthy samples (Fig. 1A). The PCA plot shows that the CS profiles in preoperative RCC samples tended to cluster as a separate group, with limited overlap with samples obtained from healthy volunteers. By contrast, the HS profile in RCC samples partly overlapped with healthy samples. However, we also observed a tail of RCC samples with a HS profile that substantially deviated from the healthy samples. This analysis suggests that there are differences in plasma CS profile between samples from healthy subjects and most RCC samples.

We used unsupervised hierarchical clustering based on the between-sample CS or HS profile correlation to validate the PCA results and to highlight the GAG properties contributing to the separation of RCC from healthy subjects (Fig. 1B). In agreement with PCA, unsupervised clustering confirmed a separation in the CS profile of healthy subjects from RCC samples. Seventeen of 19 healthy samples (89%) formed a cluster together with seven of 175 RCC samples (4%) that were markedly separated from other clusters containing 168 of 175 RCC samples (96%) and two of 19 healthy samples (11%). It is noteworthy that these other clusters displayed heterogeneous patterns of CS properties, with no single CS property being consistently higher or lower than for the group of healthy subjects. This analysis could not readily associate the diversity of patterns to RCC stage, grade, or histology. Despite this heterogeneity, in general the CS profile of RCC samples featured one or more of the following alterations: a lower fraction of unsulfated CS (0s CS); a higher fraction of 4-sulfated CS (4s CS); a higher CS charge; or a higher total CS concentration. In line with PCA, the HS profiles of healthy subjects did not form a separate group when clustering was performed together with RCC samples. However, this analysis highlighted an isolated cluster with a statistically significant enrichment of RCC samples with no healthy samples included ($p = 0.03$; proportion equality test). This cluster featured notably higher Ns HS and HS charge. We did not observe any association with stage, grade, or histology for RCC samples specifically belonging to this cluster.

3.3. Plasma GAG scores to distinguish RCC from healthy subjects

We previously developed a plasma GAG score that distinguished metastatic ccRCC from healthy subjects with AUC = 1 and 92.6% accuracy in two historical cohorts from Sweden and Italy [14]. We noted that this GAG score only partly matched the alterations observed in the present series. For example, in our previous study the Ns HS fraction was consistently low in metastatic ccRCC; here, we observed extremely high Ns HS fractions in some RCC samples. In addition, the 6s CS fraction was high in metastatic ccRCC; here, the healthy samples had 6s CS levels comparable to many RCC samples. Accordingly, the published score underperformed in this data set (80% sensitivity, 42% specificity; AUC 0.738, 95% confidence interval [CI] 0.627–0.850; Supplementary Table 1), even when Ns HS was omitted from the score calculation (AUC 0.804, 95% CI 0.705–0.904; Supplementary Fig. 2A). We observed that the performance of the published score in this data set was affected by high 6s CS fractions in the healthy group and the presence of a cluster of RCC samples with high Ns HS fraction. Were the historical healthy cohorts used as control group, the AUC for the published score would be 0.909 (95% CI 0.867–0.951) with 80% sensitivity

and 92% specificity. Omission of Ns HS from the score would achieve an AUC of 0.999 (95% CI 0.998–1; Supplementary Fig. 2B).

Therefore, we sought to redefine the formula to calculate the GAG score so that: (1) it incorporated the GAG alterations observed in the current cohort in addition to those observed in the historical Swedish and Italian cohorts; and (2) it was robust to variability in the control healthy group. To this end, we designed a discovery set comprising 67 preoperative RCC versus 19 healthy samples from the current cohort and all historical RCC and healthy samples from the two published cohorts (Swedish cohort: 26 RCC vs 20 healthy; Italian cohort: 23 RCC vs 5 healthy). The RCC samples from the current cohort represented a random selection of the total samples (38% of total preoperative RCC samples) which had been included in the interim analysis for this study. The following GAG properties were considered given their association with RCC in the current cohort or the historical cohorts: the 6s CS fraction, the 6s/4s CS ratio (normalized here by total 4s and 6s CS), the total CS concentration, the CS charge, and the 0s/Ns HS ratio (on a $\log_2$ scale to increase robustness). When adjusting for the cohort, all these properties were significantly different between RCC and healthy samples (Table 3, Fig. 2).

The final consensus formula consisted of five GAG properties:

$$\begin{aligned}\text{Plasma score} = {} & \frac{3}{10}[\text{6s CS}] + 25\frac{[\text{6s CS}]}{[\text{6s CS}] + [\text{4s CS}]} \\ & + \frac{6}{10}\text{CS}_{\text{tot}} + 13 \cdot \text{CS charge} \\ & + \frac{6}{100}\log_2\left(1 + \frac{[\text{0s HS}]}{[\text{0s HS}] + [\text{Ns HS}]}\right).\end{aligned}$$

where [6s CS] is the mass fraction of 6-sulfated CS, [4s CS] is the mass fraction of 4-sulfated CS, [Ns HS] is the mass fraction of N-sulfated HS, [0s HS] is the mass fraction of unsulfated HS, CS_{tot} is the total concentration of CS in μg/ml, and CS charge is the charge-weighted sum of all CS mass fractions.

The new plasma GAG score achieved an AUC of 0.999 (95% CI 0.997–1), with a maximum accuracy of 98.9% (1 false negative) equivalent to 94.7% specificity and 100% sensitivity at an optimal cutoff score of 0.87 (Fig. 3, Supplementary Table 1). In accordance with the analysis above, the new GAG score was elevated for all RCC samples irrespective and seemingly independently of tumor stage, grade, and histology. The new GAG score performed similarly in our historical cohorts, with AUC = 1 for the Italian cohort (23 stage IV RCC vs 5 healthy subjects; Supplementary Fig. 3) and AUC = 0.988 (95% CI 0.964–1) for the Swedish cohort (26 stage IV RCC vs 20 healthy subjects; Supplementary Fig. 3).

We then evaluated the new GAG score in the remaining group of 108 preoperative RCC samples (62% of total), which formed a validation set. Quantification of the GAG profile in these samples was performed after and blind to the formulation of the new score. RCC patients in the validation set were older (median 62 yr, IQR 55–68) than in the discovery set (median 55 yr, IQR 48–63; $p = 0.002$), but there were no other significant differences in the baseline characteristics (Supplementary Table 2). The new GAG score achieved an AUC of

0.991 (95% CI 0.977–1) in the validation set. At the prespecified cutoff, the validated sensitivity was 93.5% (Fig. 3, Supplementary Table 1). Note that the specificity could not be validated because the control healthy group was the same as in the discovery set.

3.4. Correlation between plasma GAG score and clinicopathologic features

We explored whether the new GAG score or any of its constituent GAG properties correlated with clinicopathologic features of the 175 preoperative RCC samples. The new GAG score did not exhibit a significant correlation with tumor stage, grade, size, or histology (Table 4). However, two of its constituent GAG properties showed a weak correlation with tumor size and/or histology. The CS charge was shifted towards higher values in nccRCC (9.8% mean increase; Mann-Whitney test $p = 0.05$) and was negatively correlated with tumor size ($\rho = -0.27$; $p = 0.001$ in a t test on the linear regression coefficient; Supplementary Fig. 4). The 0s/Ns HS ratio was also negatively correlated with tumor size ($\rho = -0.20$; $p = 0.008$; Supplementary Fig. 4).

The new GAG score was not significantly associated with age ($\rho = 0.04$; $p = 0.561$), gender (4.28% increase in males; $p = 0.692$), or fasting (1.4% increase with fasting; $p = 0.766$; $n = 80$ with available data [46% fasting]). Of all the constituent GAG properties, 6s CS ($\rho = 0.25$; $p < 0.001$) and 6s/4s CS ratio ($\rho = 0.25$, $p < 0.001$) showed a positive correlation with age. No other significant associations with age, gender, or fasting were observed.

3.5. Correlation of the new GAG score and its constituent properties with OS

We investigated whether the preoperative score or any of its constituent GAG properties correlated with RCC prognosis. Prognosis was first evaluated in terms of OS after surgery.

OS was computed for all 175 RCC patients. There were 19 deaths (11%) in this population over median follow-up of 53 mo (IQR 37–60). The estimated 3-yr OS was 90.4% (95% CI 85.9–95.1%). We built a univariate Cox proportional hazards model for each of the following variables: age, tumor size, tumor grade (G3/G4/high vs G2/low), tumor TNM stage (III/IV vs I/II), type of nephrectomy (radical vs partial), surgical margins (positive vs negative), Stage, Size, Grade, and Necrosis (SSIGN) score, and the new GAG score and its five constituent GAG properties (6s CS, 6s/4s CS ratio, CS_{tot}, CS charge, 0s/Ns HS ratio). Tumor size, grade, and stage, radical nephrectomy, positive surgical margins, and the SSIGN score were significantly associated with OS (Table 5). In addition, three of five GAG properties in the new GAG score were also significantly associated with OS, even though the new GAG score did not reach significance by itself (HR 1.25; $p = 0.08$). Starting from the variables significantly associated with OS in univariate analysis, we built a multivariate Cox proportional hazards model. This model was cross-validated using penalized Lasso, which returned a multivariate model consisting of four variables: tumor size, SSIGN score, surgical margins, and CS_{tot}. Of these, CS_{tot} (HR 1.51; $p < 0.001$) and SSIGN score were independent prognostic factors for OS (HR 5.04; $p < 0.001$; Table 5). The concordance index for this model was 0.934; after correction for optimism, the cross-validated C-index was 0.926.

We further investigated the possibility of grouping patients according to low versus high CS_{tot} for differential association with OS. We found an optimal cutoff of 0.914 for the preoperative CS_{tot}. Forty-one patients (23%) had a CS_{tot} above the cutoff (high CS_{tot}), while

134 belonged to the low CS_{tot} group. Kaplan-Meier survival plots for all 175 patients revealed that patients in the low group had longer OS than those in the high CS_{tot} group (HR 3.6; $p = 0.002$; Fig. 4). The 3-yr OS was 80.4% (95% CI 68–95%) for the high group and 93.4% (95% CI 89–98%) for the low CS_{tot} group. Next, we explored whether other clinical variables could be used to construct a parsimonious preoperative stratification to identify the minimum number of patients at high risk of death. Note that most variables in Table 4 are not available preoperatively, except for tumor size and age. We therefore summed CS_{tot} with the tumor size centered to 5 cm (equivalent to the cutoff used to calculate the SSIGN score) and searched for an optimal cutoff for grouping patients into low versus high risk categories. The optimal cutoff was determined to be 2.37. This cutoff assigned only 28 patients (16%) to the high risk category, and 147 patients (84%) to the low risk category. This proportion is close to the proportion of deaths observed in this cohort (11%). Accordingly, Kaplan-Meier survival plots revealed that patients in the low risk group had significantly longer OS than those in the high risk group (HR 10; $p = <0.001$; Fig. 4). The 3-yr OS was 59.2% (95% CI 43–82%) in the high risk group versus 96.2% (95% CI 93–99%) in the low risk group. We verified that this stratification reached higher statistical significance than if the stratification were solely based on tumor size ($p = 8 \times 10^{-10}$ versus $p = 9 \times 10^{-7}$) owing to the less parsimonious classification of patients in the high risk category when only tumor size is considered ($n = 71$ vs 104 patients had tumor size >5 cm). This strengthens the conclusion that CS_{tot} provides additional prognostic information for OS compared to tumor size alone. Finally, we built a multivariate Cox model using CS_{tot} and tumor size as the only preoperative variables to regress OS. The C-index for this model was 0.857; after correction for optimism, the C-index was 0. 846.

3.6. Correlation of the new GAG score and its constituent properties with RFS

We repeated the analysis above for RFS, with recurrence defined as radiological evidence of any distant metastatic lesion(s) any time after surgery.

RFS was estimated for the subset of 152 RCC patients with no evidence of distant metastases before surgery. Note that this excluded all 22 pM1 cases and one pT1N0M0 case who developed metastases between first radiological diagnosis and surgery. There were 19 recurrences (12.5%) in this population and the median follow-up was 51 mo (IQR 36–57). The estimated 3-yr RFS was 90.8% (95% CI 86–96%). We built a univariate Cox proportional hazards model for each of the variables previously considered for OS, except the SSIGN score was replaced by the Leibovich score. Tumor size, stage, radical nephrectomy, and the Leibovich score were significantly associated with RFS (Table 6). In addition, two of five GAG properties in the new GAG score as well as the new GAG score itself were also significantly associated with RFS. Starting from the variables significantly associated with RFS in univariate analysis, we built a multivariate Cox proportional hazards model. This model was cross-validated using penalized Lasso, which returned a multivariate model consisting of three variables: nephrectomy type, the Leibovich score, and CS_{tot}. The latter two were independently associated with RFS with similar prognostic value (HR 2.25 and 1.25; $p = 0.045$ and 0.054 respectively; Table 6). The C-index for this model was 0.864; after correction for optimism, the cross-validated C-index was 0. 849. In analogy to OS, we investigated if it were possible to group patients into low versus high CS_{tot} for differential

association with RFS. We found an optimal cutoff of 1 for the preoperative CS_{tot}. Twenty-one patients (14%) had CS_{tot} above the cutoff (high CS_{tot}), while 131 belonged to the low CS_{tot} group. Kaplan-Meier survival plots revealed that patients in the low CS_{tot} group had longer RFS than those in the high CS_{tot} group (HR 2.7; $p = 0.046$; Fig. 5). The 2-yr RFS was 79.1% (95% CI 63–100%) for the high CS_{tot} group versus 94.4% (95% CI 90–98%) for the low CS_{tot} group. We sought to construct a parsimonious preoperative stratification to identify the minimum number of patients at high risk of recurrence by factoring in tumor size as the only other significant clinical variable available before surgery. We thus summed CS_{tot} and the tumor size centered to 5 cm, and found an optimal cutoff of 2.05. This cutoff assigned only 34 patients (22%) to the high risk category, as opposed to 118 patients (78%) to the low risk category. This proportion is close to the proportion of recurrences observed in this cohort (12.5%). Accordingly, Kaplan-Meier survival plots revealed that patients in the low risk group had significantly longer RFS than those in the high risk group (HR 6.3; $p = <0.001$; Fig. 5). The 2-yr RFS was 78.8% (95% CI 66–94%) in the high risk group versus 96.4% (95% CI 93–100%) in the low risk group. We also verified in this case that the proposed stratification reached higher statistical significance than if the stratification were solely based on tumor size ($p = 9 \times 10^{-5}$ vs. $p = 6 \times 10^{-4}$) possibly owing to the less parsimonious classification of patients in the high risk category when only tumor size is considered ($n = 49$ vs 103 patients had tumor size >5 cm). As in the case of OS, we built a multivariate Cox model using CS_{tot} and tumor size as the only preoperative variables to regress RFS. The C-index for this model was 0.762; after correction for optimism, the C-index was 0.742.

3.7. Change in the new GAG score and its constituent properties after surgery

We finally investigated whether the new GAG score changed after surgery. Of the 152 patients with at least one postoperative sample, 139 had RCC at pathologic evaluation. For this analysis, we computed the change in new GAG score for each RCC patient between the preoperative samples and the first available postoperative sample. This difference in new GAG score was widely variable across patients, with an increase in score observed for 53% of cases and a decrease for 47% after surgery. The direction of change did not seem to correlate with patient outcomes as assessed by evidence of recurrence within 2 yr from surgery (Supplementary Fig. 5).

To test whether the lack of coherent GAG score changes after surgery was attributable to technical noise in the measurement of the plasma GAG profile, we replicated the GAG measurements in a quasi-random subset of 40 pairs of postoperative and preoperative RCC samples for a total of 80 samples assessed in duplicate. The reproducibility of the new GAG score across the 80 duplicates was moderately high, with a coefficient of variation (CV) of 18.5% ± 15%. Importantly, all 40 preoperative samples in the second batch were correctly classified as RCC and not healthy given that the corresponding new GAG score was always above the prespecified cutoff (Supplementary Fig. 6). However, the correlation between the new GAG scores for the 80 samples in the first versus the second batch was low, mainly because most of the RCC samples had scores in a narrow range. The preoperative versus postoperative difference in GAG score was sensitive to this low correlation between batches and yielded no correlation in the direction of change before and after surgery between the

two batches (odds ratio 0.7; $p = 0.75$). This lack of coherent changes can probably be explained by the fact that measurement errors are compounded when calculating a difference between GAG scores as opposed to calculating the absolute GAG score, for which the reported CV was 18.5%. Overall, this analysis seems to indicate that the new GAG score does not normalize after surgery, even though a conclusive experiment should be conducted once the technical variability in the measurement of plasma GAGs is sufficiently low.

4. Discussion

In this study, we profiled plasma GAGs in preoperative samples from a retrospective consecutive series of 175 RCC patients referred for surgery to investigate whether plasma GAGs are diagnostic and prognostic in nonmetastatic RCC. We report that a new GAG score, developed on the basis of our previously published GAG score for metastatic ccRCC [14], had 93.5% sensitivity and 94.7% specificity for discriminating RCC from healthy samples, with the sensitivity estimate independently validated among 108 RCC patients. The new GAG score was independent and uncorrelated to tumor stage, grade, size, and histology, and was not confounded by either age or gender. One of the constituent properties in the new GAG score, namely CS_{tot}, was an independent prognostic factor for OS and RFS. When combined with tumor size, the only other significant clinical variable available preoperatively, CS_{tot} provided a tool for parsimonious stratification of patients as having high versus low risk for metastatic recurrence or death, with high concordance.

These results expand our knowledge on the diagnostic and prognostic potential of plasma GAGs in RCC, which was so far limited to metastatic ccRCC in our previous studies [14,15]. Other groups reported that GAGs are significantly altered in RCC tissue compared to normal adjacent tissues, confirming the role of the tumor in altering the concentration and composition of GAGs [23–25]. Although previous studies revealed alterations in GAG concentrations in urine from patients with localized RCC [25,26], there is very limited information on the effects of RCC on GAG compositions and, to the best of our knowledge, no other studies on the effects of RCC on GAG concentrations and compositions in plasma. This is partly explained by the complexity of plasma GAG extraction and subsequent laboratory characterization. Indeed, it is only recent technical advances in the field [27–29] that helped to identify changes in plasma and urine GAG profiles in other noncancerous pathologies such as septic shock [30] and respiratory failure [31]. However, the infancy of these advances explains the lack of standardized assays commercially available, which may have implications for the results presented here, as further discussed below.

Our study revealed some unanticipated observations regarding plasma GAGs in RCC patients. We observed little to no correlation between the GAG properties used to compute the new GAG score and tumor stage, grade, and histology. This seems to indicate that the changes in these plasma GAG properties are not entirely induced by the tumor. Simply put, a larger tumor burden did not translate into larger changes in these GAG properties. In addition, these GAG properties appeared to be extremely sensitive to very small tumors in this cohort, in which 39% of RCC patients had a tumor of <4 cm in size. From a biophysical perspective, it seems unlikely that such small tumors are able to affect and maintain the observed GAG alterations in human circulation. An alternative hypothesis is that an external

factor could respond to RCC at its earliest inception—hence the exceptional sensitivity—and that this factor is partly responsible for GAG alterations. Such a response might be elicited by the stroma or the immune system, given their association with plasma GAG changes in previous studies [32,33]. Another hypothesis is that these GAG alterations might originate from the tumor and that the liver maintains plasma GAG homeostasis [34,35] despite changes in the tumor burden. However, this hypothesis clashes with the observation that GAG scores did not seem to decrease postoperatively, even though most samples were taken 4 wk after surgery, which might not be sufficient to capture fluctuations after surgery. (For example, prostate-specific antigen testing after radical prostatectomy in prostate cancer is recommended between 6 and 8 wk after surgery.) On the contrary, an immune/stromal response might well be active for months after surgery and justify the persistence of the new GAG score. In our previous study, we observed that GAG scores decreased to normal levels in eight patients with no evidence of disease, but these samples were obtained years after the first surgery. If we assume that the GAG changes observed resulted mostly because of an external factor, this would make plasma GAGs a less-than-ideal biomarker according to conventional criteria because it might affect specificity to RCC [36]. However, the requirement that ideal biomarkers should originate from the tumor in order to maximize specificity has historically yielded poor sensitivity for low-stage tumors, as recently shown [37]. Low specificity has obvious repercussions if biomarkers are to be applied for early cancer detection or differential diagnosis, but their high sensitivity could be useful for other applications important in the clinical management of RCC, such as surveillance for recurrence after surgery.

It has been shown that plasma GAGs have potential to compensate for the lack of minimally invasive biomarkers in the management of RCC [38] in both nonmetastatic and metastatic settings. Other biomarkers have shown promising results in RCC, such as urinary aquaporin-1 (AQP1) and perlipin-2 (PLIN2) [39–41]. These urinary proteins had ≥ 95% sensitivity and ≥ 91% specificity for RCC compared to patients undergoing routine abdominal computed tomography [41]. AQP1 and PLIN2 changes seem to originate specifically from RCC [39,41]. It is unknown if AQP1 and PLN1 levels are independent prognostic factors in RCC, as observed here for plasma GAGs. Plasma GAG scores and urinary AQP1 and PLN1 seem to be complementary in their utility as optimally sensitive and specific minimally invasive biomarkers.

Despite the clear potential of the GAG score as a biomarker of direct clinical use, this study has limitations. Retrospective sample collection may affect GAG concentrations and composition, in that it is unknown whether sample age is an important factor for GAG stability. Moreover, slight differences in the sampling protocol compared to our previous study may have resulted in noise in the GAG measurements. For example, we previously centrifuged samples at 2500 × *g* for 15 min at 4 °C, while the current samples were centrifuged at 1100 × *g* for 10 min at room temperature, and it is known that a difference in centrifugal force affects metabolome estimates [42]. Another source of noise is the current unavailability of commercial assays for standardized assessment of plasma GAGs. This noise is probably compensated by the large sample size and by the fact that all measurements were performed in a single laboratory. Nevertheless, the presence of noise warrants validation of the study conclusions in a prospective cohort with standardized

procedures. Finally, we observed differences between the healthy population in this study and that in our previous study. Unfortunately, there is no comprehensive and systematic evaluation of physiological levels of plasma GAGs in the literature. Most studies rely on small sample sizes and our study represents the largest characterization of plasma GAGs in human samples. It is possible that differences in ethnicity and lifestyle can lead to different plasma GAG baseline levels in different populations, as seen in this American cohort when compared to the Swedish and Italian cohorts in our previous study. This hypothesis seems corroborated by the fact that Schmidt et al [31] observed a healthy GAG profile among American volunteers that was more similar to the healthy group in the present study, while Mantovani et al [33] observed a healthy GAG profile among Italian volunteers that was more similar to the healthy group in our previous study. Despite these baseline differences, we observed substantial plasma GAG changes in RCC that were robust to different populations. A comprehensive evaluation of plasma GAGs in a large healthy population is nevertheless required. Finally, the multivariate analysis suggests that pre-surgical plasma GAGs are associated with metastatic recurrence independent of tumor stage and thereby could be used to identify high risk patients across stage groups. However, the cohort was not powered to validate whether such association would be still significant in the subset of RCC with high-stage disease.

5. Conclusions

The results presented here indicate that plasma GAG levels can provide accurate diagnostic and prognostic information that may have clinical utility in the management of nonmetastatic RCC. Plasma GAG alterations appear to originate as a response to the tumor and occur early if not concomitantly with tumor formation, and probably independent of its progression. This warrants prospective studies on clinical applications for which the simplicity of blood-based biomarkers and the sensitivity of GAGs can contribute to extending or improving the survival outlook for RCC patients.

Supplementary Material

Refer to Web version on PubMed Central for supplementary material.

Acknowledgments:

The authors wish to thank Brandon Manley and Maria Becerra at the Memorial Sloan Kettering Cancer Center for help in the collection of clinical data and John K. Kruschke for advice on Bayesian statistics.

***Funding/Support and role of the sponsor*:** This work was financially supported by the Knut and Alice Wallenberg Foundation to Chalmers University of Technology and MSK Cancer Center Support Grant P30-CA008748 to the Memorial Sloan Kettering Cancer Center. The sponsors played no direct role in the study.

Financial disclosures: Jens Nielsen certifies that all conflicts of interest, including specific financial interests and relationships and affiliations relevant to the subject matter or materials discussed in the manuscript (eg, employment/affiliation, grants or funding, consultancies, honoraria, stock ownership or options, expert testimony, royalties, or patents filed, received, or pending), are the following: At the start of the study, Francesco Gatto and Jens Nielsen were listed as co-inventors on patent applications related to the biomarkers described in this study. At the time of manuscript submission, Francesco Gatto and Jens Nielsen were shareholders in Elypta AB, which owned the above-mentioned patent applications, Francesco Gatto was an employee of Elypta AB and Jens Nielsen was chairman of the board. The remaining authors have nothing to disclose.

References

[1]. Ferlay J, Soerjomataram I, Dikshit R, et al. Cancer incidence and mortality worldwide: sources, methods and major patterns in GLOBOCAN 2012. Int J Cancer 2015;136:E359–86. [PubMed: 25220842]

[2]. Hsieh JJ, Purdue MP, Signoretti S, et al. Renal cell carcinoma. Nat Rev Dis Primers 2017;3:17009. [PubMed: 28276433]

[3]. Belldegrun AS, Klatte T, Shuch B, et al. Cancer-specific survival outcomes among patients treated during the cytokine era of kidney cancer (1989–2005): a benchmark for emerging targeted cancer therapies. Cancer 2008;113:2457–63. [PubMed: 18823034]

[4]. Dabestani S, Thorstenson A, Lindblad P, et al. Renal cell carcinoma recurrences and metastases in primary non-metastatic patients: a population-based study. World J Urol 2016;34:1081–6. [PubMed: 26847337]

[5]. Kuijpers YA, Meijer RP, Jonges GN, et al. Potentially curable recurrent disease after surgically managed non-metastatic renal cell carcinoma in low-, intermediate- and high-risk patients. World J Urol 2016;34:1073–9. [PubMed: 27055532]

[6]. Dabestani S, Beisland C, Stewart GD, et al. Long-term outcomes of follow-up for initially localised clear cell renal cell carcinoma: RECUR database analysis. Eur Urol Focus 2018. 10.1016/j.euf.2018.02.010.

[7]. Finley DS, Pantuck AJ, Belldegrun AS. Tumor biology and prognostic factors in renal cell carcinoma. Oncologist 2011;16(Suppl 2):4–13. [PubMed: 21346035]

[8]. Jonasch E, Futreal PA, Davis IJ, et al. State of the science: an update on renal cell carcinoma. Mol Cancer Res 2012;10:859–80. [PubMed: 22638109]

[9]. Moch H, Srigley J, Delahunt B, et al. Biomarkers in renal cancer. Virchows Arch 2014;464:359–65. [PubMed: 24487793]

[10]. Hakimi AA, Reznik E, Lee CH, et al. An integrated metabolic atlas of clear cell renal cell carcinoma. Cancer Cell 2016;29:104–16. [PubMed: 26766592]

[11]. Creighton CJ, Morgan M, Gunaratne PH, et al. Comprehensive molecular characterization of clear cell renal cell carcinoma. Nature 2013;488:43–9.

[12]. Gatto F, Nookaew I, Nielsen J. Chromosome 3p loss of heterozygosity is associated with a unique metabolic network in clear cell renal carcinoma. Proc Natl Acad Sci U S A 2014;111:E866–75. [PubMed: 24550497]

[13]. Wettersten HI, Hakimi AA, Morin D, et al. Grade-dependent metabolic reprogramming in kidney cancer revealed by combined proteomics and metabolomics analysis. Cancer Res 2015;75:2541–52. [PubMed: 25952651]

[14]. Gatto F, Volpi N, Nilsson H, et al. Glycosaminoglycan profiling in patients' plasma and urine predicts the occurrence of metastatic clear cell renal cell carcinoma. Cell Rep 2016;15:1822–36. [PubMed: 27184840]

[15]. Gatto F, Maruzzo M, Magro C, et al. Prognostic value of plasma and urine glycosaminoglycan scores in clear cell renal cell carcinoma. Front Oncol 2016;6:253. [PubMed: 27933273]

[16]. Volpi N, Galeotti F, Yang B, et al. Analysis of glycosaminoglycan-derived, precolumn, 2-aminoacridone-labeled disaccharides with LC-fluorescence and LC-MS detection. Nat Protoc 2014;9:541–58. [PubMed: 24504479]

[17]. Galeotti F, Coppa GV, Zampini L, et al. Capillary electrophoresis separation of human milk neutral and acidic oligosaccharides derivatized with 2-aminoacridone. Electrophoresis 2014;35:811–8. [PubMed: 24338619]

[18]. Kottler R, Mank M, Hennig R, et al. Development of a high-throughput glycoanalysis method for the characterization of oligosaccharides in human milk utilizing multiplexed capillary gel electrophoresis with laser-induced fluorescence detection. Electrophoresis 2013;34:2323–36. [PubMed: 23716415]

[19]. Zhang Z, Murtagh F, Van Poucke S, et al. Hierarchical cluster analysis in clinical research with heterogeneous study population: highlighting its visualization with R. Ann Transl Med 2017;5:75. [PubMed: 28275620]

[20]. Tibshirani R Regression shrinkage and selection via the Lasso. J R Stat Soc Ser B Methodol 1996;58:267–88.

[21]. Kruschke JK. Bayesian estimation supersedes the t test. J Exp Psychol Gen 2013;142:573–603. [PubMed: 22774788]

[22]. Kruschke JK. Doing Bayesian data analysis: a tutorial with R, JAGS, and Stan. ed. 2 Boston, MA: Academic Press; 2015.

[23]. Ucakturk E, Akman O, Sun X, et al. Changes in composition and sulfation patterns of glycoaminoglycans in renal cell carcinoma. Glycoconj J 2016;33:103–12. [PubMed: 26662466]

[24]. Salanti A, Clausen TM, Agerbaek MO, et al. Targeting human cancer by a glycosaminoglycan binding malaria protein. Cancer Cell 2015;28:500–14. [PubMed: 26461094]

[25]. Batista LT, Matos LL, Machado LR, et al. Heparanase expression and glycosaminoglycans profile in renal cell carcinoma. Int J Urol 2012;19:1036–40. [PubMed: 22738382]

[26]. Sarica K, Turkolmez K, Soygur T, et al. Evaluation of urinary glycosaminoglycan excretion in patients with renal cell carcinoma. Eur Urol 1997;31:54–7. [PubMed: 9032535]

[27]. Sun X, Li L, Overdier KH, et al. Analysis of total human urinary glycosaminoglycan disaccharides by liquid chromatography-tandem mass spectrometry. Anal Chem 2015;87:6220–7. [PubMed: 26005898]

[28]. Lawrence R, Olson SK, Steele RE, et al. Evolutionary differences in glycosaminoglycan fine structure detected by quantitative glycan reductive isotope labeling. J Biol Chem 2008;283:33674–84. [PubMed: 18818196]

[29]. Wei W, Ninonuevo MR, Sharma A, et al. A comprehensive compositional analysis of heparin/heparan sulfate-derived disaccharides from human serum. Anal Chem 2011;83:3703–8. [PubMed: 21473642]

[30]. Schmidt EP, Overdier KH, Sun X, et al. Urinary glycosaminoglycans predict outcomes in septic shock and ARDS. Am J Respir Crit Care Med 2016;194:439–49. [PubMed: 26926297]

[31]. Schmidt EP, Li GY, Li LY, et al. The circulating glycosaminoglycan signature of respiratory failure in critically ill adults. J Biol Chem 2014;289:8194–202. [PubMed: 24509853]

[32]. Shao C, Shi XF, White M, et al. Comparative glycomics of leukocyte glycosaminoglycans. FEBS J 2013;280:2447–61. [PubMed: 23480678]

[33]. Mantovani V, Galeotti F, Maccari F, et al. Analytical methods for assessing chondroitin sulfate in human plasma. J AOAC Int 2016;99:333–41. [PubMed: 26961813]

[34]. Pecly IM, Melo-Filho NM, Mourao PA. Effects of molecular size and chemical structure on renal and hepatic removal of exogenously administered chondroitin sulfate in rats. Biochim Biophys Acta 2006;1760:865–76. [PubMed: 16545912]

[35]. Guimaraes MA, Mourao PA. Urinary excretion of sulfated polysaccharides administered to Wistar rats suggests a renal permselectivity to these polymers based on molecular size. Biochim Biophys Acta 1997;1335:161–72. [PubMed: 9133653]

[36]. Duffy MJ. Role of tumor markers in patients with solid cancers: a critical review. Eur J Intern Med 2007;18:175–84. [PubMed: 17449388]

[37]. Cohen JD, Li L,Wang Y, et al. Detection and localization of surgically resectable cancers with a multi-analyte blood test. Science 2018;359:926–30. [PubMed: 29348365]

[38]. Pastore AL, Palleschi G, Silvestri L, et al. Serum and urine biomarkers for human renal cell carcinoma. Dis Markers 2015;2015:251403. [PubMed: 25922552]

[39]. Morrissey JJ, Mobley J, Song J, et al. Urinary concentrations of aquaporin-1 and perilipin-2 in patients with renal cell carcinoma correlate with tumor size and stage but not grade. Urology 2014;83, 256.e9–14.

[40]. Morrissey JJ, Mobley J, Figenshau RS, et al. Urine aquaporin 1 and perilipin 2 differentiate renal carcinomas from other imaged renal masses and bladder and prostate cancer. Mayo Clin Proc 2015;90:35–42. [PubMed: 25572193]

[41]. Morrissey JJ, Mellnick VM, Luo J, et al. Evaluation of urine aquaporin-1 and perilipin-2 concentrations as biomarkers to screen for renal cell carcinoma: a prospective cohort study. JAMA Oncol 2015;1:204–12. [PubMed: 26181025]

[42]. Lesche D, Geyer R, Lienhard D, et al. Does centrifugation matter? Centrifugal force and spinning time alter the plasma metabolome. Metabolomics 2016;12:159. [PubMed: 27729833]

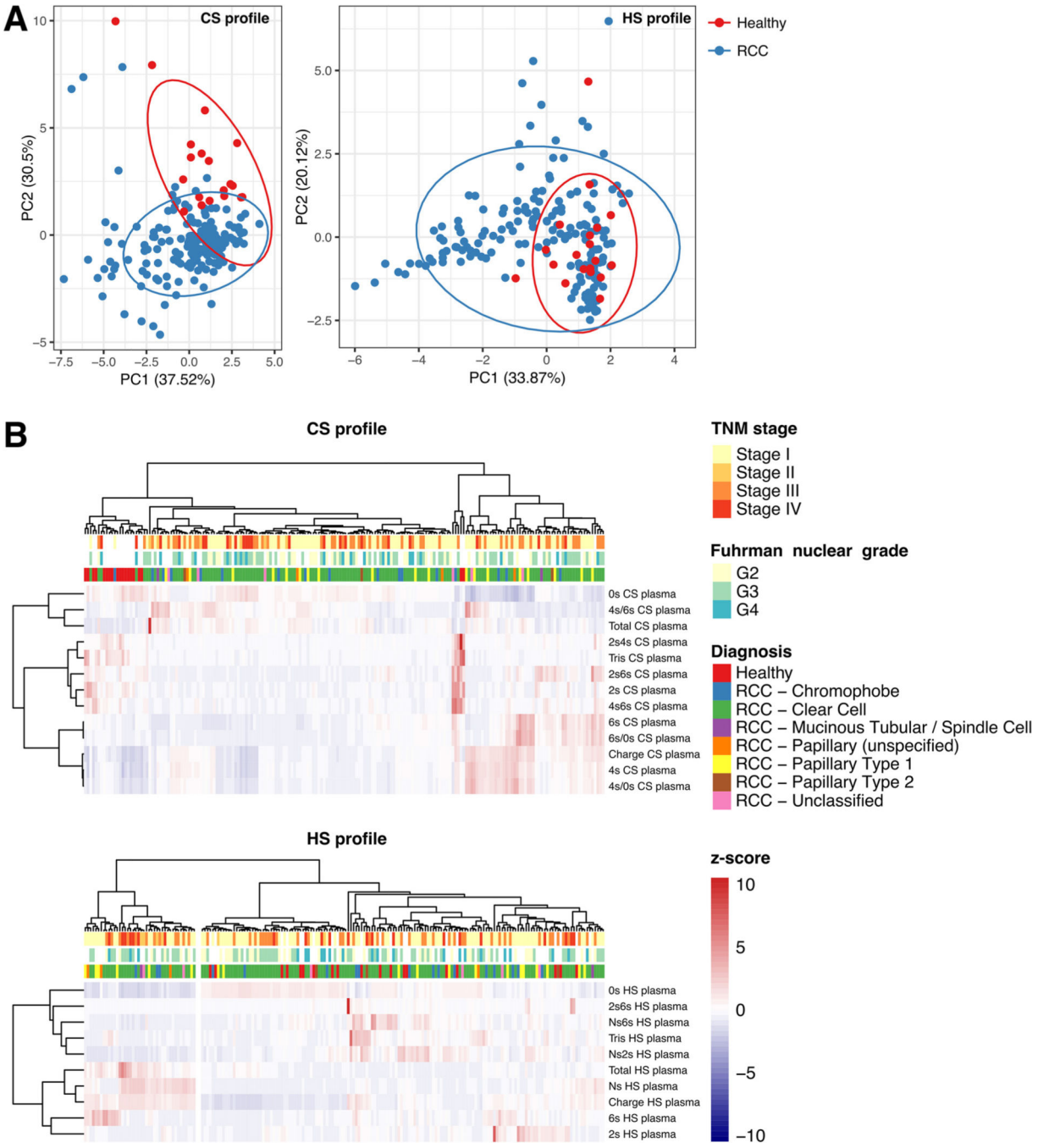

Fig. 1 –.

Clustering analysis of plasma chondroitin sulfate (CS) and heparan sulfate (HS) profiles for 175 preoperative renal cell carcinoma (RCC) samples and 19 samples from healthy subjects. (A) Principal component analysis (PCA) based on quantification of the CS and HS profile in plasma samples from RCC patients and healthy subjects. Each point represents an individual sample. The percentage indicates the proportion of variance explained along the axis of each principal component (PC). The ellipses delimit the area in which samples belonging to a certain group are expected to be located at a 95% confidence level assuming a multivariate *t*

distribution. (B) Unsupervised hierarchical clustering based on between-sample correlation in the CS and HS profiles. Each row represents an individual CS or HS property. Each column represents a sample. The annotation above provides information on the principal diagnosis, the Fuhrman nuclear grade (if applicable and available) and the TNM stage. For each row, values for the corresponding CS or HS property were normalized as *z* scores.

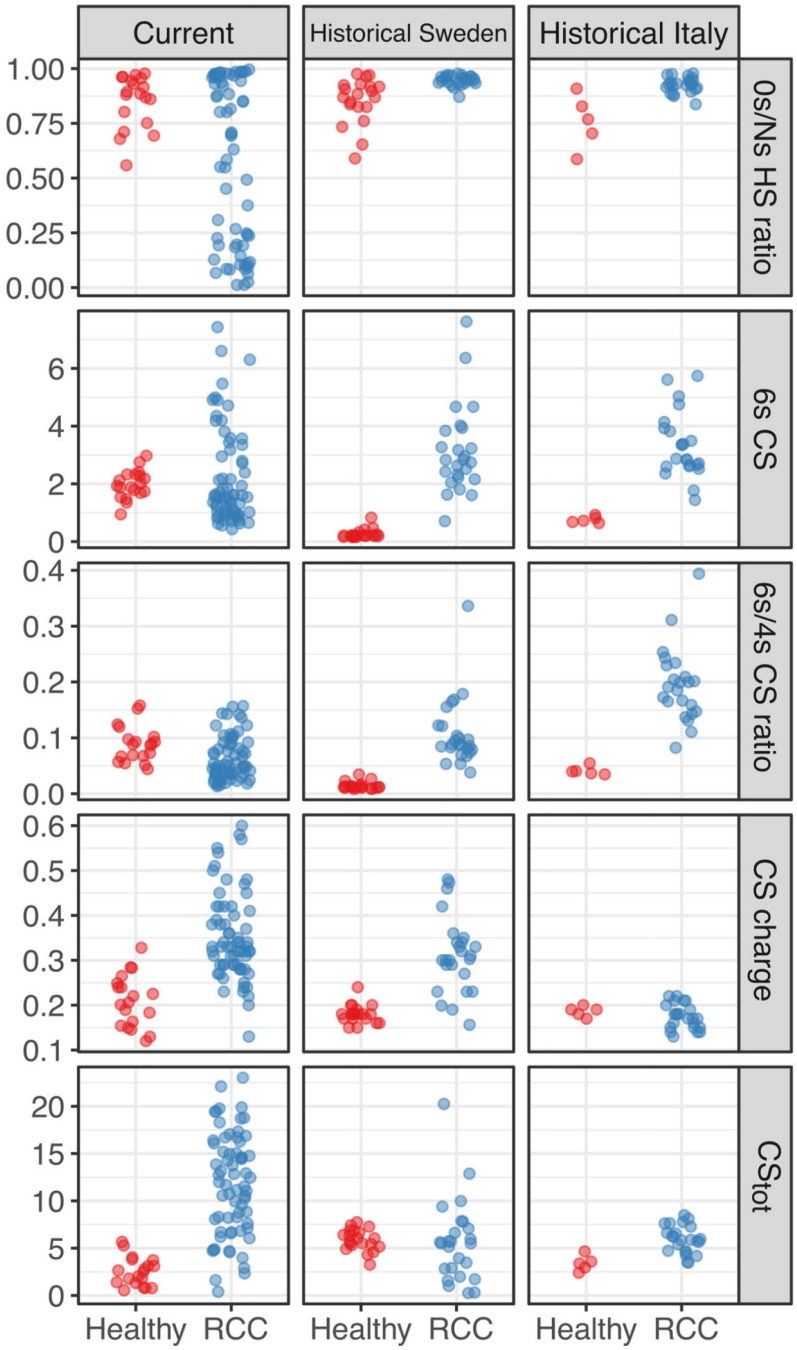

Fig. 2 –.

Selected glycosaminoglycan properties in plasma samples in the discovery set, comprising 38% of the current cohort (RCC 67, healthy 19) and two historical cohorts from Sweden (RCC 26, healthy 20) and Italy (RCC 23, healthy 5) [14]; see also Table 3. RCC = renal cell carcinoma; CS = chondroitin sulfate; HS = heparan sulfate; tot = total.

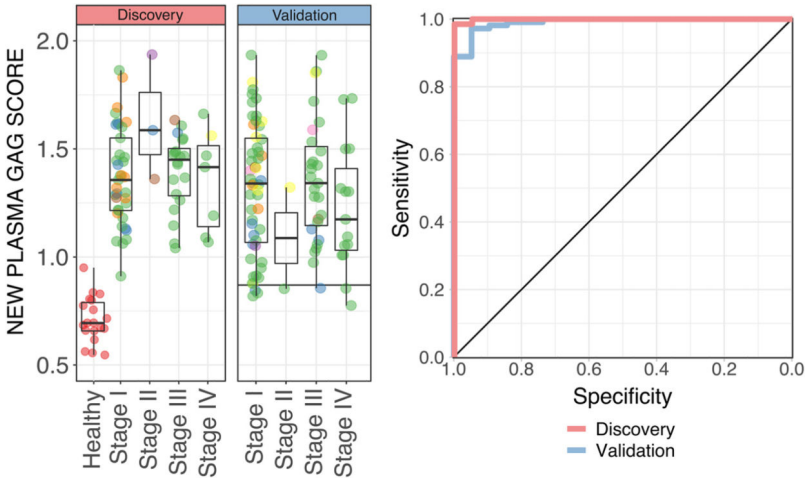

Fig. 3 –.

(A) Boxplot of the new plasma glycosaminoglycan (GAG) score for 19 healthy samples versus 67 preoperative renal cell carcinoma (RCC) samples comprising the discovery set versus 108 preoperative RCC samples comprising the validation set. The horizontal line indicates the cutoff score corresponding to maximum accuracy for the discovery set. (B) Corresponding receiver operating characteristic curve for classification for the discovery and validation sets. Note that 12 samples with scores greater than 2 in the validation set were omitted from display to prevent shrinkage of the plot.

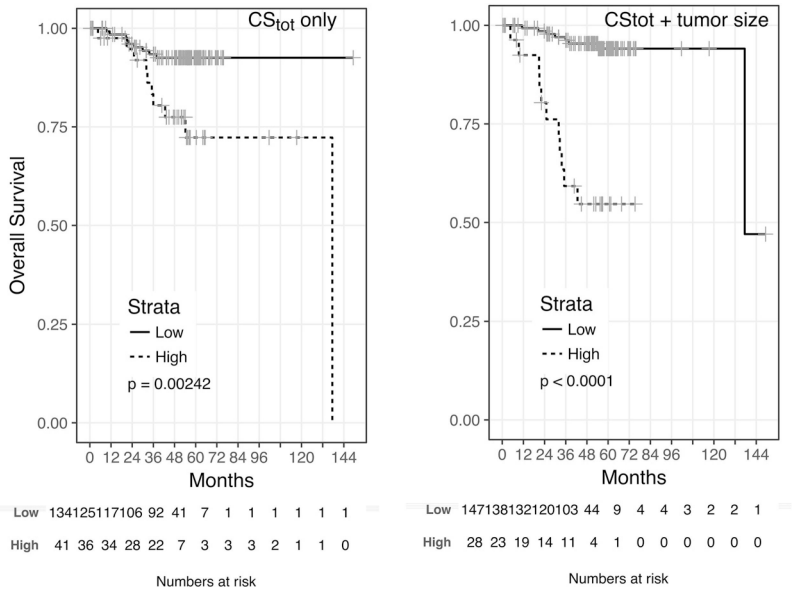

Fig. 4 –.

Kaplan-Meier curves for overall survival for low versus high risk according to (A) the preoperative total chondroitin sulfate (CS_{tot}) value alone and (B) the preoperative CS_{tot} value combined with tumor size >5 cm among 175 patients with renal cell carcinoma.

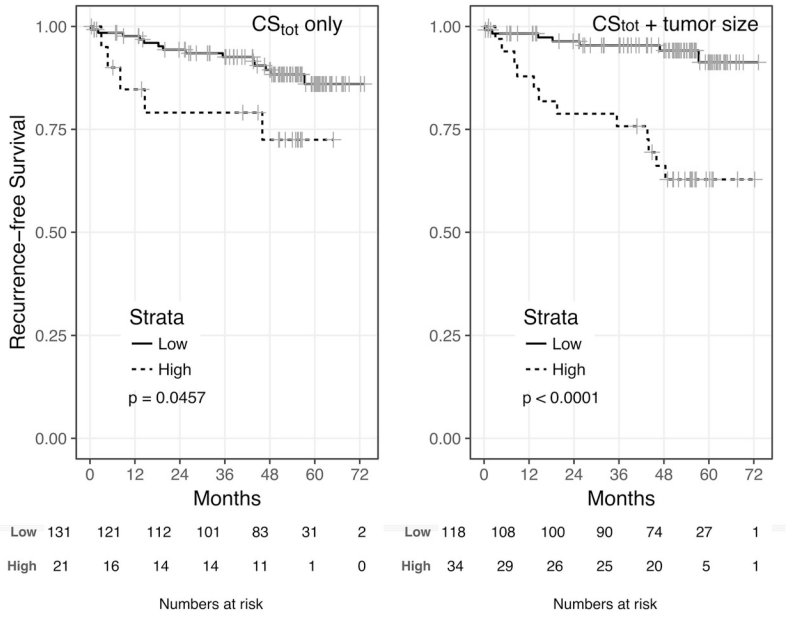

Fig. 5 –.

Kaplan-Meier curves for recurrence-free survival for low versus high risk according to (A) the preoperative total chondroitin sulfate (CS_{tot}) value alone and (B) the preoperative CS_{tot} combined with tumor size >5 cm among 152 patients with nonmetastatic renal cell carcinoma.

Table 1 –

Demographic and clinicopathological characteristics of the retrospective cohort of patients and healthy volunteers

Characteristic	Patients (*n* = 194)	Healthy (*n* = 19)
Median age, yr (interquartile range)	60 (52–67)	55 (50–60)
Gender (*n*)		
Female	60	13
Male	134	6
Race (*n*)		
White	174	0
African American	9	0
Asian American	3	0
Other/not available	8	19
Diagnosis (*n*)		
Renal cell carcinoma	175	
Oncocytoma	7	
Angiomyolipoma	6	
Urothelial cell carcinoma	3	
Other benign	2	
Other malignant	1	

Table 2 –

Demographic and clinicopathological characteristics of the subcohort of patients with renal cell carcinoma (RCC)

Characteristic	RCC (*n* = 175)
Median age, yr (interquartile range)	60 (52–67)
Gender (*n*)	
Female	48
Male	127
Ethnicity (*n*)	
White	159
African American	7
Asian American	2
Other/not available	7
Histological subtype (*n*)	
Clear cell	124
Non–clear cell	51
Chromophobe	17
Mucinous tubular and spindle cell	2
Papillary type I	19
Papillary type II	3
Papillary (unspecified)	4
Unclassified	6
Median tumor size, cm (interquartile range)	4.5 (2.9–7)
pT stage (*n*)	
T1	94
T1a	70
T1b	24
T2	7
T2 (unspecified)	3
T2a	2
T2b	2
T3	72
T3 (unspecified)	3
T3a	57
T3b	11
T3c	1
T4	1
Not available	1
pN stage (*n*)	
N0	61
N1	7
NX	107

Characteristic	**RCC (*n* = 175)**
pM stage (*n*)	
M0	152
M1	22
Not available	2
TNM stage, (*n*)	
Stage I	94
Stage II	6
Stage III	52
Stage IV	22
Not available	1
Grade (*n*)	
Not available	35
Fuhrman nuclear grade	122
2	39
3	61
4	22
Other grading system	18
High	7
Low	11

Table 3 –

Difference in selected GAG properties between RCC (n = 116) and healthy samples (n = 44) from the discovery set (across three cohorts) according to Bayesian estimation

GAG property	MD (95% HDI)	Effective MCMC samples	MCMC samples in ROPE (%) [a]
6s CS	1.59 (0.92–2.29)	23 010	0.01
6s/(4s + 6s) CS	0.08 (0.06–0.10)	22 228	0.03
CS_{tot}	6.04 (1.80–7.78)	19 045	0.02
CS charge	0.13 (0.11–0.16)	11 857	0.00
$\log_2\left(\frac{0s}{Ns+0s}HS\right)$	0.12 (0.04–0.22)	13 189	2.35

GAG = glycosaminoglycan; RCC = renal cell carcinoma; MD = modal difference between RCC and healthy samples; HDI = high-density interval; MCMC = Markov chain Monte Carlo; ROPE = region of practical equivalence; CS = chondroitin sulfate; HS = heparan sulfate.

[a] Differences for which the fraction of MCMC samples in ROPE was below 5% are considered statistically significant.

Table 4 –

Correlation between the new plasma GAG score or any of its constituent GAG properties with clinicopathological features in preoperative RCC (N = 175) or ccRCC in the case of FNG (n = 121)

GAG property	Stage		FNG		Size in cm (n = 175)		Histology	
	LA/A (n = 80) vs localized (n = 94)		≥G3 (n = 82) vs G2 (n = 39)				nccRCC (n = 51) vs ccRCC (n = 124)	
	Shift	p value	Shift	p value	ρ	p value	Shift	p value
6s CS	−0.0006	0.8836	0.0060	0.4261	−0.1365	0.0717	−0.0060	0.3460
6s/(4s + 6s) CS	0.0097	0.5221	0.0132	0.4591	−0.0361	0.6357	−0.0285	0.0784
CS_{tot}	0.0377	0.5349	−0.1003	0.0956	0.1353	0.0742	0.0697	0.2889
CS charge	−0.0260	0.1658	0.0129	0.6873	−0.2685	0.0003	0.0389	0.0496
$\log_2\left(\frac{0s}{Ns+0s}HS\right)$	−0.0002	0.1311	−0.0002	0.1205	−0.1991	0.0083	−0.0003	0.0707
New GAG score	0.0044	0.9242	−0.0689	0.2734	0.0355	0.6413	0.0770	0.1788

GAG = glycosaminoglycan; RCC = renal cell carcinoma; cc = clear cell; ncc = non–clear cell; FNG = Fuhrman nuclear grade; LA/A = locally advanced or advanced; CS = chondroitin sulfate; HS = heparan sulfate.

Table 5 –

Association of clinical factors with overall survival in the preoperative renal cell carcinoma population ($n = 175$) [a]

Factor	*N* [*n* deaths]	Univariate		Multivariate	
		HR (95% CI)	*p* value	HR (95% CI)	*p* value
Age	175	1.23 (0.76–1.98)	0.391		
Tumor size	175	2.53 (1.77–3.62)	<0.001	1.13 (0.56–2.29)	0.723
Tumor grade					
Grade 2 or low	50 [2]	1			
Grade >2 or high	90 [14]	8.42 (1.11–6.41)	0.039		
Not available	35				
TNM stage					
I or II	101 [3]	1			
III or IV	74 [16]	11.67 (2.68–5.08)	0.001		
Nephrectomy type					
Partial	113 [2]	1			
Radical	62 [17]	34.8 (4.6–261.6)	<0.001		
Surgical margins					
Negative	170 [16]	1			
Positive	5 [3]	5.18 (2.12–12.6)	<0.001	4.06 (0.75–22)	0.105
SSIGN score	118	3.37 (2.21–5.13)	<0.001	5.04 (2.53–10)	<0.001
New GAG score	175	1.25 (0.97–1.62)	0.080		
6s CS	175	0.35 (0.14–0.91)	0.032		
6s/(4s + 6s) CS	175	0.62 (0.34–1.14)	0.125		
CS_{tot}	175	1.34 (1.11–1.62)	0.002	1.51 (1.19–1.93)	<0.001
CS charge	175	0.44 (0.24–0.80)	0.008		
$\log_2\left(\frac{0s}{Ns+0s}HS\right)$	175	0.80 (0.52–1.22)	0.293		

HR = hazard ratio; CI = confidence interval; GAG = glycosaminoglycan; SSIGN = Stage, Size, Grade, and Necrosis; CS = chondroitin sulfate; HS = heparan sulfate.

[a] In multivariate analysis, patients with missing data for any of the selected covariates were omitted ($n = 57$). Continuous variables were centered to the mean and scaled to the standard deviation.

Table 6 –

Association of clinical factors with recurrence-free survival in the preoperative population with nonmetastatic renal cell carcinoma ($n = 152$) [a]

Factor	*N* [*n* deaths]	Univariate		Multivariate	
		HR (95% CI)	*p* value	HR (95% CI)	*p* value
Age	152	1.54 (0.76–1.98)	0.085		
Tumor size	152	1.74 (1.77–3.62)	0.001		
Tumor grade					
Grade 2 or low	47 [3]	1			
Grade >2 or high	71 [13]	3.15 (1.11–6.41)	0.073		
Not available	34	–			
TNM stage					
I or II	98 [4]	1			
III or IV	54 [15]	7.74 (2.68–5.08)	<0.001		
Nephrectomy type					
Partial	111 [5]	1			
Radical	41 [14]	8.48 (3.05–23.6)	<0.001	1.23 (0.70–16.7)	0.130
Surgical margins					
Negative	149 [18]	1			
Positive	3 [2]	2.75 (0.66–11.5)	0.165		
Leibovich score	98	3.26 (2.21–5.13)	<0.001	2.25 (1.01–5.02)	0.045
New GAG score	152	1.34 (0.97–1.62)	0.013		
6s CS	152	0.78 (0.14–0.91)	0.376		
6s/(4s + 6s) CS	152	0.84 (0.34–1.14)	0.489		
CS_{tot}	152	1.37 (1.11–1.62)	0.003	1.31 (1.00–1.57)	0.054
CS charge	152	0.83 (0.24–0.80)	0.447		
$\log_2\left(\frac{0s}{Ns+0s}HS\right)$	152	0.67 (0.52–1.22)	0.045		

HR = hazard ratio; CI = confidence interval; GAG = glycosaminoglycan; RCC = renal cell carcinoma; CS = chondroitin sulfate; HS = heparan sulfate.

[a] In multivariate analysis, patients with missing data for any of the selected covariates were omitted ($n = 54$). Continuous variables were centered to the mean and scaled to the standard deviation.